Electronic Supplementary Material (ESI) for Materials Horizons.
This journal is © The Royal Society of Chemistry 2019

Supporting Information

Dispersed Nano-MOFs via a Stimuli-Responsive Biohybrid-System with Enhanced Photocatalytic Performance

Hui-Chun Lee,[a] *Tobias Heil,*[a] *Jian-Ke Sun,*[a,b,]* *and Bernhard V. K. J. Schmidt,*[a,]*

[a] Department of Colloid Chemistry, Max Planck Institute of Colloids and Interfaces, 14424 Potsdam, Germany

[b] School of Chemistry and Chemical Engineering, Beijing Institute of Technology, Beijing 102488, PR China

Keywords: nanoMOFs, dispersion, stimuli responsive polymer, switchable catalysis

* To whom all correspondence should be addressed.

E-mail:bernhard.schmidt@mpikg.mpg.de; jiankesun15@gmail.com

Experimental Section

Materials. 2-(Dimethylamino)ethyl methacrylate (DMAEMA, Sigma Aldrich, 98%) was passed through a basic aluminum oxide (Brockman type I, Acros, 50-200 µm, 60 Å) column to remove the inhibitor. Acetic acid (Merck, 100% anhydrous for analysis), acetone (J.T.Baker, HPLC grade), 1,2,4-benzenetricarboxylic acid (H_3btc, Sigma-Aldrich, ≥ 99%), α-bromoisobutyryl bromide (BIBB, Sigma Aldrich, 98%), 3-bromo-1-propanol (Sigma Aldrich, 97%), 4-pentyn-1-ol (Alfa Aesar, 97%), $Co(NO_3)_2{\cdot}6H_2O$ (Sigma-Aldrich, ≥ 99.9%), $CuBr_2$ (Alfa Aesar, 99%), copper(II) acetate monohydrate (Roth, ≥ 98%), $Cu(NO_3)_2{\cdot}3H_2O$ (Sigma-Aldrich, ≥ 99.9%), diazabicyclo[2.2.2]octane (dabco, Alfa Aesar, 97%), dichloromethane (DCM, Sigma-Aldrich, HPLC grade), diethyl ether (Sigma-Aldrich, ACS grade), 2,5-dihydroxyterephtalic acid (H_4dobdc, Sigma-Aldrich, 98%), *N*,*N*-dimethylformamide (DMF, VWR, ACS grade), ethanol (J.T.Baker, HPLC grade), methanol (MeOH, Fisher Scientific, for analysis), (3-mercaptopropyl)trimethoxysilane (MPTS, Sigma-Aldrich, 95%), 2-methylimidazole (Hmim, Sigma-Aldrich, 99%), sodium azide (Roth, ≥ 98%), 1,4-terephthalic acid (H_2bdc, Alfa Aesar, >98%), triethylamine (TEA, Acros, 99%), 4- 1,1,4,7,7-pentamethyldiethylentriamine (PMDETA, Acros, > 98%), pentyn-1-ol (Alfa Aesar, 97%), Rhodamine B (RhB, Sigma Aldrich, 97%), $K_2S_2O_8$ (Sigma Aldrich, 99.9%), toluene (J.T.Baker, HPLC grade), tetrahydrofuran (THF, VWR, HPLC grade) $Zn(NO_3)_2{\cdot}6H_2O$ (Sigma Aldrich, ≥98%) and $Zn(OAc)_2{\cdot}2H_2O$ (Sigma-Aldrich, 99.9%), were used as received. Rape pollen grains were purchased from Yier Biofarm (Shandong, China), washed intensively with KOH, acetic acid and methanol to remove the intine layer; the washed pollen was dried at ambient temperature, and stored at 4 ºC.[1] As light source, a 50 W LED chip (Bridgelux BXRA-50C5300; λ > 410 nm) connected to a home-made circuit and cooling system is utilized. The emission spectrum is shown in Figure S19.

Characterization. The microstructure of the MOFs was characterized by a Bruker D8 powder X-ray diffractometer (PXRD) using Cu-Kα radiation (λ = 0.154 nm) and a scintillation counter (KeveX Detector). The observations of field-emission scanning electron microscopy (FE-SEM) were performed on a LEO 1550 Gemini instrument. Samples were located on carbon coated aluminum holder, and measured without any additional coating. The UV-vis spectra were recorded on UV-2501PC/2550 (Shimadzu Corporation, Japan) at ambient temperature. Residual copper in click products was determined by inductively coupled plasma optical emission spectrophotometry (ICP-OES). The measurements were performed on Perkin Elmer Optima 8000, calibrated with standard solutions. Gas chromatography-mass spectrometry (GC-MS) analysis was performed using an Agilent Technologies 5975 gas chromatograph equipped with a MS detector and a capillary column (HP-5MS, 30 m, 0.25 mm, 0.25 micron) for conversion determination. The solvent-dependent particle size of grafted PDMAEMA brushes was measured by dynamic light scattering (DLS). The measurements were performed on Zetasizer Nano ZS90 (Malvern) with $\lambda = 633$ nm at $\theta = 90°$ and polystyrene as absorption reference. All ^{1}H nuclear magnetic resonance (NMR) spectra were performed on a Bruker Ascend 400 NMR spectrometer in chloroform-*d* at a concentration of 1 wt%. Size exclusion chromatography (SEC) for PDMAEMA was conducted in NMP (Fluka, GC grade) with 0.05 mol/L LiBr and BSME as internal standard at 70 °C using a column system by PSS GRAM 100/1000 column (8 × 300 mm, 7 μm particle size) with a PSS GRAM precolumn (8 × 50 mm), a Shodex RI-71 detector, and a PMMA calibration with standards from PSS. The molar dispersity is defined as $Đ = M_w/M_n$. The theoretical number averaged molecular mass $M_{n,theo}$ was calculated as $MM_{initiator} + MM_{monomer} \times ([\text{monomer}]_0/[\text{initiator}]_0) \times \text{conversion}$.

Synthesis of Initiator-Functionalized Silane (MPTS-Br). According to the literature,[2] α-bromoisobutyryl bromide (5.92 g, 25.7 mmol, 1.0 equiv) was added dropwise to a solution of

3-(mercaptopropyl)trimethoxysilane (5.03 g, 25.6 mmol, 1.0 equiv) and triethylamine (2.59 g, 25.6 mmol, 1.0 equiv) in dry toluene (42.5 mL) in an ice-bath under stirring. The mixture was stirred overnight at ambient temperature. The salt was removed by filtration, and the remaining solution was removed under reduced pressure to give the initiator 2-bromothioisobutyrate (MPTS-Br) for grafting (85% yield). ^{1}H NMR (400 MHz, $CHCl_3$): δ = 3.57 (9H, $SiOCH_3$), 2.95 (2H, SCH_2), 1.97 (6H, $C(CH_3)_2Br$), 1.74 (2H, CCH_2C), 0.78 (2H, CH_2Si) (Figure S20).

Synthesis of 3-Azido-Propanol. According to the literature,[3] sodium azide (4.60 g, 70.8 mmol, 1.5 equiv) was placed in a 250 mL flask and dissolved in a mixture of acetone (72 mL) and deionized water (12.0 mL). 3-Bromo-1-propanol (3.92 mL, 44.8 mmol, 1.0 equiv) was added, and the mixture was refluxed overnight. Acetone was evaporated under reduced pressure at ambient temperature, and then deionized water (60 mL) was added. The aqueous phase was extracted with diethyl ether (3 x 60 mL). The extracted organic mixture was dried over anhydrous magnesium sulfate. The solvent was removed under reduced pressure to give 3-azido-1-propanol as a yellow oil (3.81 g, 37.7 mmol, 84% yield). ^{1}H NMR (400 MHz, $CHCl_3$): δ = 3.72 (t, 2H, CH_2OH), 3.43 (t, 2H, N_3-CH_2), 1.82 (p, 2H, N_3-CH_2CH_2) (Figure S21).[3, 4]

Preparation of PDMAEMA-Functionalized Pollens (*P*-pollen). Typically, the washed pollen (0.1 g) was immersed in a solution of the MPTS-Br (5 wt%) in toluene (10 mL), and the mixture was gently refluxed for 24 h. The MPTS-Br functionalized pollen was washed with toluene (3 x 10 ml) and dried under vacuum at ambient temperature. After the initiator-functionalized pollen was fabricated, SI-ARGET ATRP was carried out to graft PDMAEMA from the pollen surface. DMAEMA (0.5 g, 31.75 mmol, 5670 equiv.), $CuBr_2$ (1.3 mg, 5.6 μmol, 1.0 equiv.), PMDETA (2.3 mg, 13.0 μmol, 2.3 equiv.), dabco (12.0 mg, 0.11 mmol, 19.6 equiv.) and anhydrous methanol (0.5 ml) were introduced into a 5 mL vial and mixed well. Then the 5% initiator-functionalized pollen (0.5 g) was added into the mixture, and the polymerization was conducted at 65 ºC for 24 h with conversion 98%. The PDMAEMA-grafted pollen (*P*-pollen) was washed and re-suspended in DCM (0.91 g, ~93% yield). The grafted PDMAEMA brushes were cut from *P*-pollens by 1% NaOH, and characterized by ^1H NMR (400 MHz, $CHCl_3$): δ = 4.04 (2H, OCH_2), 2.55 (2H, CH_2N), 2.26 (6H, $N(CH_3)_2$), 2.05-1.63 (2H, CH_2C main chain), 1.42-0.73 (3H, CCH_3), and SEC: M_n = 67800 g/mol ($Đ$ = 1.2) (Figure S22).

Fabrication of $Cu_2(bdc)_2(dabco)$. $Cu_2(bdc)_2(dabco)$ was employed to catalyze the photocatalytic reactions demonstrated in this study. The $Cu_2(bdc)_2(dabco)$ was prepared under solvothermal condition.[5] $Cu(NO_3)_2{\cdot}3H_2O$ (0.29 g, 1.2 mmol), terephthalic acid (0.21 g, 1.2 mmol) and dabco (0.07 g, 0.6 mmol) was dissolved separately in DMF (15 ml). The terephthalic acid solution was first added into the copper salt mixture, and then the dabco solution was added. The mixture was stirred at ambient temperature for 1 h before thermal treatment (85 ºC for 24 h). The mixture was cooled down spontaneously. Non-coordinated molecules and smaller nanocrystals were removed by washing with DMF and DCM (3 × wash and a day per time), giving $Cu_2(bdc)_2(dabco)$ powder (0.43 g, yield ~75%). The as-synthesized $Cu_2(bdc)_2(dabco)$ was further characterized with FESEM and PXRD (Figure 1) and then remained in DCM before utilization (Note: the MOF nanocrystals are seriously aggregated and precipitated in DCM, similarly hereinafter the MOFs below). As shown in Figure 1c, the PXRD with high resemblance between the as-fabricated MOF and the simulation indicates the formation of same microstructures and pure crystalline phase. In principle, MOF nanocrystals with extremely small size might be detached from the surface due to enhanced dispersibility in DCM and swollen PDMAEMA brushes. However, triple one-day long DCM washing of the MOF crystals was performed during synthesis in order to remove small DCM dispersible $Cu_2(bdc)_2(dabco)$ crystals. Consequently, only MOF crystals which are large enough and non-detachable were used in the synthesis of $Cu_2(bdc)_2(dabco)$@*P*-pollen composite. A similar procedure was applied to other MOF@*P*-pollen composites.

Fabrication of $Zn_2(bdc)_2(dabco)$. The $Zn_2(bdc)_2(dabco)$ was synthesized under solvothermal condition.[6] $Zn(NO_3)_2{\cdot}6H_2O$ (0.36 g, 1.2 mmol), terephthalic acid (0.21 g, 1.2 mmol) and dabco (0.07 g, 0.6 mmol) was dissolved separately in DMF (15 ml). The terephthalic acid solution was first added into the zinc salt mixture, and then the dabco solution was added. The mixture was stirred at ambient temperature for 1 h before thermal treatment (85 ºC for 24 h). The mixture was cooled down spontaneously. After removing the non-coordinated molecules by washing with DMF and DCM (3 × wash and a day per time), the $Zn_2(bdc)_2(dabco)$ MOF was obtained (0.34 g, yield ~53%). The synthesized MOF was characterized with FESEM and PXRD (Figure S6) and then remained in DCM before utilization.

Fabrication of MOF-5-Zn. The MOF-5-Zn was synthesized according to literature at ambient temperature.[7-9] terephthalic acid (0.5 g, 3 mmol) and TEA (0.85 mL) were dissolved in 40 mL of DMF. $Zn(OAc)_2{\cdot}2H_2O$ (1.7 g, 7.7 mmol) was dissolved in 50 mL of DMF, and then added to the organic mixture stirring overnight. The forming precipitate was collected by centrifugation, and after removing the non-coordinated molecules by washing with DMF and DCM (3 × wash and a day per time), the MOF-5 was obtained (1.18 g, yield ~57%). The as-synthesized MOF-5 was characterized with FESEM and PXRD (Figure S6) and remained in DCM before utilization.

Fabrication of MOF-74-Zn. The MOF-74-Zn was synthesized according to literature at ambient temperature.[7] H_4dobdc (0.24 g, 1.2 mmol) and $Zn(OAc)_2{\cdot}2H_2O$ (0.69 g, 3.1 mmol) was dissolved separately in 20 mL DMF. Then the ligand solution was added into the zinc salt solution, and the mixture was stirred overnight. The forming precipitate was collected by centrifugation, and after removing the non-coordinated molecules by washing with DMF and

DCM (3 × wash and a day per time), the MOF-74-Zn was obtained (0.59 g, yield ~64%). The as-synthesized MOF-74-Zn was characterized with FESEM and PXRD (Figure S6) and remained in DCM before utilization.

Fabrication of Cu(bdc). The Cu(bdc) was synthesized by solvothermal condition according to literature.[10, 11] terephthalic acid (0.167 g, 1.0 mmol) and $Cu(NO_3)_2·3H_2O$ (0.24 g, 1.0 mmol) was dissolved separately in 10 mL DMF. The metallic solution was pour into the ligand solution stirring at ambient temperature for 2 h, and then the mixture was refluxed at 100 °C for 2 days. The forming precipitate was collected by centrifugation, and after removing the non-coordinated molecules by washing with DMF and DCM (3 × wash and a day per time), the Cu(bdc) was obtained (0.30 g, yield ~73%). The synthesized MOF was characterized with FESEM and PXRD (Figure S6) and remained in DCM before utilization.

Fabrication of HKUST-1. The HKUST-1[6] was synthesized according to literature.[3] H_3btc (0.5 g, 2.4 mmol) and $Cu(OAc)_2·H_2O$ (0.86 g, 4.31 mmol) was dissolved separately in 12 mL DMF-ethanol-water mixture (volume ratio = 1:2:3). The metallic solution was pour into the ligand solution stirring at ambient temperature overnight. The forming precipitate was collected by centrifugation, and after removing the non-coordinated molecules by washing with DMF and DCM (3 × wash and a day per time), the HKUST-1 was obtained (0.99 g, yield ~73%). The synthesized MOF was characterized with FESEM and PXRD (Figure S6) and remained in DCM before utilization.

Fabrication of ZIF-67. The ZIF-67 was synthesized according to literature.[12] Hmim (5.5 g, 0.067 mol) was dissolved in 20 mL water, and $Co(NO_3)_2·6H_2O$ (0.45 g, 1.54 mmol) was dissolved in 3 mL water separately. The metallic solution was pour into the ligand solution stirring at ambient temperature overnight. The forming precipitate was collected by centrifugation, and after removing the non-coordinated molecules by washing with water, methanol and DCM (3 × wash and a day per time), the ZIF-67 was obtained (4.58 g, yield

~77%). The synthesized MOF was characterized with FESEM and PXRD (Figure S6) and remained in DCM before utilization.

Incorporation of MOFs on *P*-pollen (MOFs@*P*-pollen). DCM, one of the good solvents for PDMAEMA, was employed as the reaction medium in which the polymer chains were highly stretched, enabling efficient association between functional groups from comprised monomers and MOF crystals. Take $Cu_2(bdc)_2(dabco)$@*P*-pollen as an example, the as-synthesized *P*-pollen (0.1 g) was first suspended in DCM (10 ml), and then $Cu_2(bdc)_2(dabco)$ (0.1 g) was added. The mixture was gently shaken overnight. The non-incorporated MOF crystals were removed by low-speed centrifugation, and the suspension was dried under reduced pressure at ambient temperature, giving the $Cu_2(bdc)_2(dabco)$@*P*-pollen complex (0.13 g, ~70% yield). The as-prepared complexes were characterized by PXRD and FESEM (Figure 1 and S6) comparing to the native MOF. The incorporated amount of each MOF in the MOF@*P*-pollen composite was determined by ICP-OES using the comprised metallic ions in individual MOF framework, giving yield between 61 and 79% (Table S1).

$Cu_2(bdc)_2(dabco)$-mediated Photo-CuAAC reaction. The given amount of $Cu_2(bdc)_2(dabco)$ was utilized to catalyze the click reaction under visible light in DCM or toluene. Typically, $Cu_2(bdc)_2(dabco)$ (2.0 mg) was added to the mixture of 4-pentyn-1-ol (0.231 g, 2.75 mmol, 1.0 equiv), 3-azido-1-propanol (0.275 g, 2.75 mmol, 1.0 equiv) and solvent (0.5 ml). After 30 min stirring, the click reaction was carried out by exposing the reaction mixture to a 50 W visible-light LED in a distance of 15 cm. The conversion at a given time was determined by GC-MS. Alternatively referring to the reaction condition catalyzed by native $Cu_2(bdc)_2(dabco)$, $Cu_2(bdc)_2(dabco)$@*P*-pollen (7.1 mg) and $Cu_2(bdc)_2(dabco)$@PDMAEMA (0.133 g) were utilized separately as different types of $Cu_2(bdc)_2(dabco)$ composite to catalyze the photo-CuAAC reaction.

Repeated Photo-CuAAC reaction in DCM and toluene. The given amount of $Cu_2(bdc)_2(dabco)$@*P*-pollen (7.1 mg) was utilized to catalyze photo-CuAAC reaction in DCM and Toluene alternatively referring to the reaction condition in $Cu_2(bdc)_2(dabco)$-mediated photo-CuAAC reaction, and the reaction was three times repeated for each solvent. The conversion of the given cycle was determined by GC-MS, and yield was measured by the weight of obtained triazole product. After each reaction, $Cu_2(bdc)_2(dabco)$@*P*-pollen was washed with methanol (3 x 5 ml), dried under vacuum at ambient temperature, and then utilized for the next reaction. The temporally-controlled photo-CuAAC reaction in DCM/toluene mixed solvents was first started in pure DCM mixture (0.3 g CuAAC reagents). After a given reaction time the reaction was centrifuged to remain the catalysts in the vial bottom before each measurement, and two-third of the DCM mixture (i.e. 0.2 g) was removed and utilized for conversion analysis. Then, fresh CuAAC reagents in toluene (0.2 g) was added to the remained DCM mixture (0.1 g), forming the toluene-dominant mixture with the same mass of 0.3 g for next reaction. Following this strategy, the catalysis was repeatedly conducted in DCM or toluene-dominated mixed solvents. As a result, the concentration of catalyst is consistent throughout the reaction, and only the comprised solvent ratio is changed, by which the accessibility of catalytic sites on $Cu_2(bdc)_2(dabco)$@*P*-pollen corresponding to environment was traced. The cumulative conversion was determined by summing up the conversion resulted from each round, illustrating the adjustable catalytic property of $Cu_2(bdc)_2(dabco)$@*P*-pollen.

$Cu_2(bdc)_2(dabco)$-Mediated Photodegradation of Rhodamine B (RhB). The same amount of $Cu_2(bdc)_2(dabco)$ coming from innate MOF or $Cu_2(bdc)_2(dabco)$@*P*-pollen was utilized to degrade RhB under visible light in DCM or toluene. Typically, RhB (1.1 mg) and $K_2S_2O_8$ (0.027 g) were dissolved in water/methanol (1.2 ml, 1:1 volume ratio), and then $Cu_2(bdc)_2(dabco)$ (2.5 mg) or $Cu_2(bdc)_2(dabco)$@*P*-pollen (8.8 mg) as well as the test solvent

(3 ml) were add to the mixture. The dye degradation reaction was carried out by exposing the reaction mixture to a 50 W visible-light LED in a distance of 15 cm with continuous stir. The conversion rate at the given time was determined by UV-Vis based on the absorbance at 554 nm which was assigned to RhB. All the mixtures are filtered by the PTFE filter with pore size of 0.45 μm before analysis to remove the solid catalyst. The potassium persulfate, $K_2S_2O_8$, was added to conduct the photolysis of RhB. Under visible light irradiation the MOF-comprised Cu(II) can be reduced to Cu(I) and convert one $K_2S_2O_8$ molecule to two strong oxidizing radicals, $\cdot SO_4^-$. Due to the high reduction potential of $\cdot SO_4^-$ the dye contamination will be efficiently oxidized and decomposed.[13]

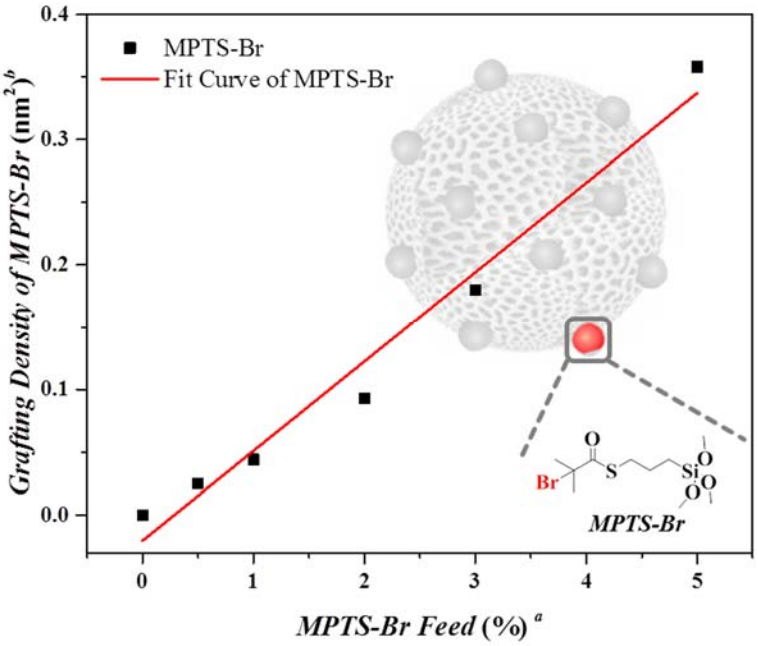

Figure S1. Grafting density of grafted initiator, MPTS-Br, on pollen grains (σ_{Br}). ^{a} The feed concentration of MPTS-Br within the initial solution. ^{b} Determined via ICP-OES with Br element, and BET method[14, 15] giving pollen surface area (after removing the internal complex) of 6.8 m^2/g. Note: following the reference, before utilization the purchased rape pollen grains are washed intensively with KOH, acetic acid and methanol to remove the intine layer. Therefore, only the exine, outer and robust shell, is remained and utilized as supporting pivot for grafted polymer brushes.[1]

Calculated Grafting Density. The grafting density of grafted PDMAEMA chains (σ_p) on pollen can be assessed by Equation S1:

$$\boldsymbol{\sigma_p = \sigma_{Br} f_{ini} = \frac{(grafted\ amount\ of\ initiator) \times f_{ini}}{(surface\ area\ of\ pollen)}} \qquad (\boldsymbol{S1})$$

where $\boldsymbol{\sigma_p}$ is grafting density of polymer brush, $\boldsymbol{\sigma_{Br}}$ is grafting density of grafted initiator on pollen grains which is obtained from ICP-OES result in Figure S1 and $\boldsymbol{f_{ini}}$ is initiation efficiency of polymerization. In this study, 5% MPTS-Br was applied to prepare the PDMAEMA-functionalized pollen (i.e. *P*-pollen) and to demonstrate the following dispersibility and catalytic tests. The M_n = 67800 g/mol and $Đ$ = 1.2 of grafted PDMAEMA was characterized by SEC (Figure S22). Due to the controlled molecular weight by using ARGET ATRP, with conversion = 99%, the theoretical molecular weight, M_{theo}, of grafted PDMAEMA was calculated to be 30400 g/mol. Therefore, the initiation efficiency of PDMAEMA grafted on *P*-pollen was determined by $M_{n,Theo}$ / $M_{n,SEC}$, giving initiation efficiency (f_{ini}) = 44.8%.

$$\boldsymbol{\sigma_p = 0.716 \times 44.8\% = 0.32\ chain/nm^2}$$

Due to the high grafting density of PDMAEMA brushes (σ_p = 0.32 chain/nm^2), the space between each chain is around 3.1 nm. It is possible that MOF crystals with hundred-nanometer particle size could be presented on the outer surface of pollens as well as in the interior chamber. Nevertheless, considering the condensed grafted polymer brushes and the particle size of the applied $Cu_2(bdc)_2(dabco)$ which is much larger than 3.1 nm, the MOF crystals could mainly exist on the surface.

Exponential Scaling Behavior. The extended chain length of grafted polymer brushes can be estimated by Equation S2:

$$\boldsymbol{h \propto N\sigma_p^n} \qquad\qquad (\boldsymbol{S2})$$

where h is the average length of extended brushes (layer thickness), N is the degree of polymerization, σ_p is the grafting density of polymer brushes and n is an exponent correlated to solvent, grafting density and molecular properties. A higher grafting density ($\sigma_p \geq 0.3$ nm^{-2}) is a core factor for responsive polymers in extended chain conformation, which contributes to increased steric hindrance. [16, 17]

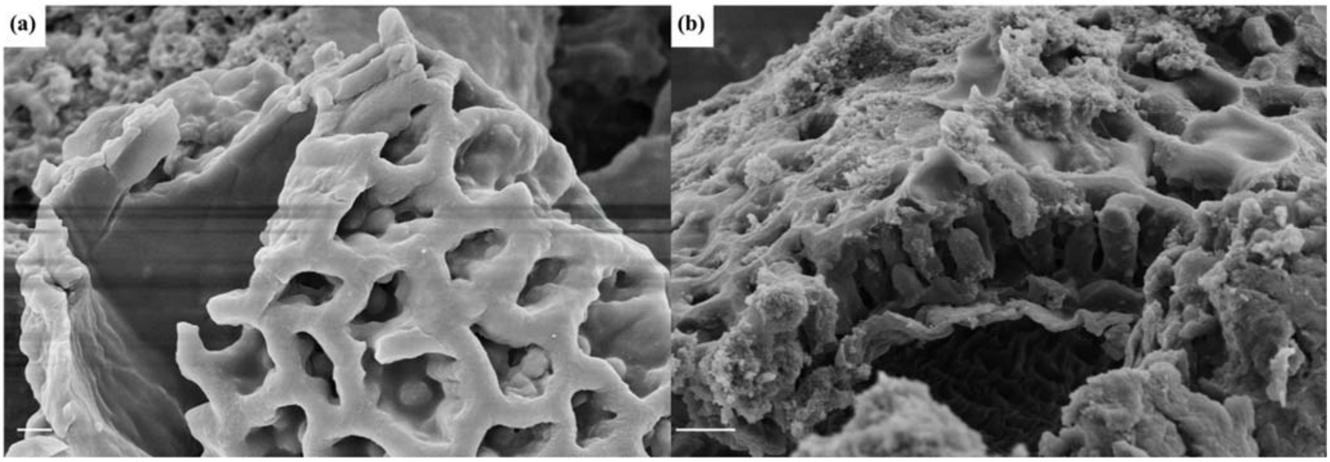

Figure S2. FE-SEM cross section images of (a) innate pollen and (b) $Cu_2(bdc)_2(dabco)$@*P*-pollen with the hierarchical hollow structures. The scale bar is shown with 1 μm.

Table S1. Incorporated Amount of MOF [a] in the MOF@*P*-pollen composites [b]

	Type of Metallic Ion	Amount of Metallic Ion (mg/g)	Incorporated MOF (wt%)
MOF-74-Zn	Zn	99.2	24.6
MOF-5		155	23.0
$Zn_2(bdc)_2(dabco)$		113	24.9
$Cu_2(bdc)_2(dabco)$	Cu	62.9	28.3
Cu(bdc)		58.5	36.4
HKUST-1		55.3	17.5
ZIF-67	Co	65.4	24.5
$Cu_2(bdc)_2(dabco)$@ PDMAEMA [c]	Cu	3.37	1.5

[a] Determined via ICP-OES. [b] The M_n = 67800 g/mol (degree of polymerization: ~ 431) and $Đ$ = 1.2 of grafted PDMAEMA was characterized by SEC. Due to the controlled molecular weight by using ARGET ATRP, with conversion = 99%, the theoretical molecular weight, M_{theo}, of grafted PDMAEMA was calculated to be 30400 g/mol. Therefore, the initiation efficiency of PDMAEMA grafted on *P*-pollen was determined by $M_{n,Theo}$ / $M_{n,SEC}$, giving initiation efficiency (f_{ini}) = 44.8%. [c] The PDMAEMA brushes cut from *P*-pollen were utilized directly as the free-formed polymer chains to incorporate $Cu_2(bdc)_2(dabco)$ nanocrystals.

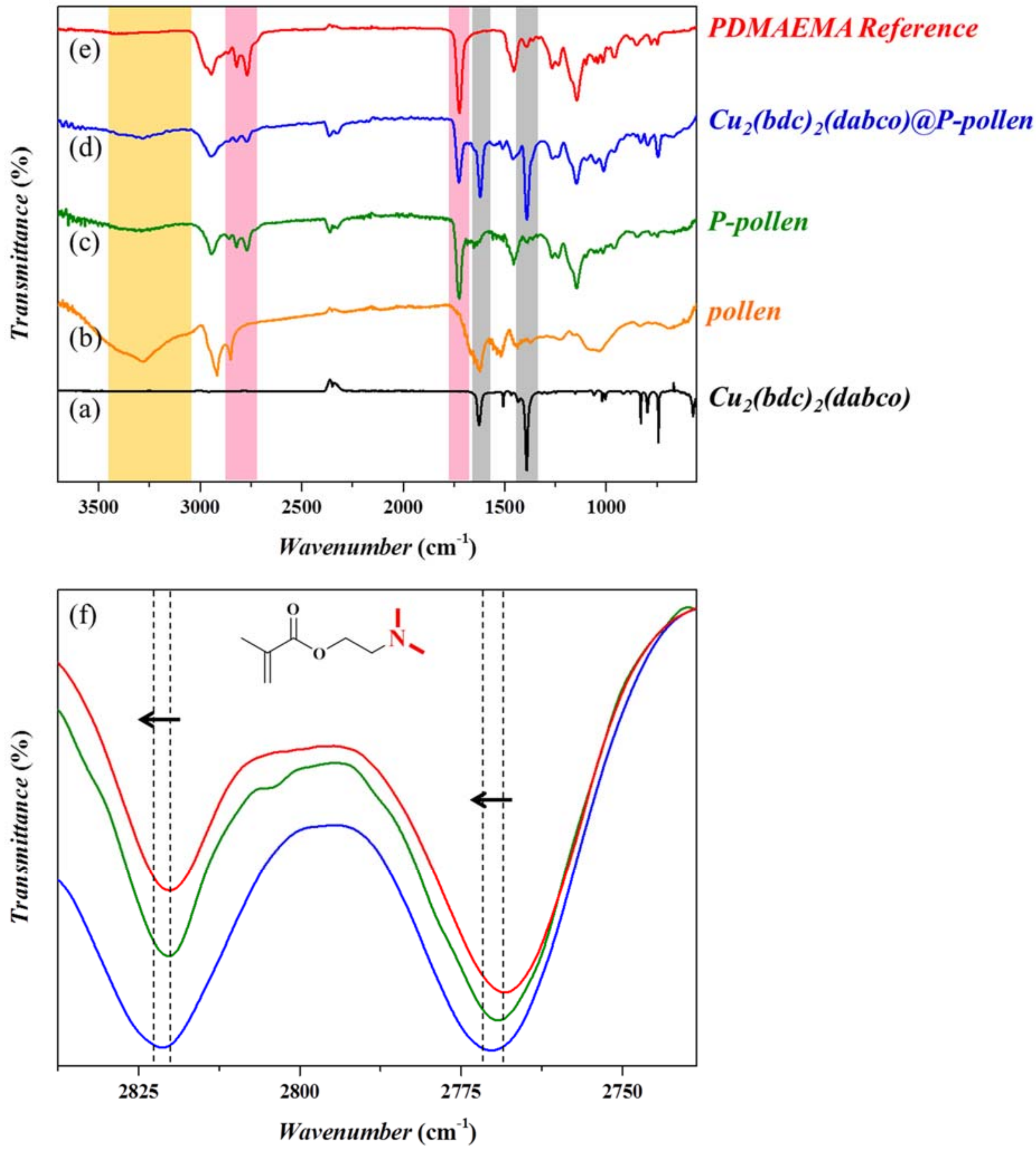

Figure S3. ATR-FTIR spectra: (a) as-synthesized $Cu_2(bdc)_2(dabco)$, (b) pollen, (c) *P*-pollen, (d) $Cu_2(bdc)_2(dabco)$@*P*-pollen, (e) PDMAEMA reference and (f) the magnified N-H band of (c), (d) and (e). Note: the colored curves in (f) denote the same compounds in figure c-e. The shift of N-H stretching band (2768 and 2819 cm^{-1}) towards higher wavenumbers (2819 and 2823 cm^{-1}) after incorporation of $Cu_2(bdc)_2(dabco)$ indicated the direct association between PDMAEMA and MOF nanocrystals.

Calculated Crystal Size from PXRD. The crystal size of as-synthesized MOF can be calculated by the PXRD using Debye-Scherrer equation:

$$\boldsymbol{D}_{\mathrm{p}} = \frac{\boldsymbol{k\lambda}}{\boldsymbol{\beta \cos \theta}} \qquad (\boldsymbol{S3})$$

where $\boldsymbol{D}_{\mathbf{p}}$ stands for average crystal size, k is Scherrer constant (0.94 for spherical crystals with cubic symmetry), λ is X-ray wavelength (0.154 nm for Cu-Kα), β is full width at half maximum (FWHM) and θ is peak position.[18, 19] Based on the PXRD profiles in Figure 1c, the average crystal size of as-synthesized $Cu_2(bdc)_2(dabco)$ and $Cu_2(bdc)_2(dabco)$*P*-pollen is around 85 nm and 75 nm separately, which is consistent with the FESEM image.

Calculated Optical Band Gap. The interaction between MOF and *P*-pollen was further traced by solid-state UV-Vis spectroscopy to evaluate individual optical band gap, E_G, by the Tauc equation (Equation S4):

$$(\boldsymbol{\alpha h v})^{2} = \boldsymbol{A}(\boldsymbol{hv} - \boldsymbol{E_G}) \qquad (\boldsymbol{S4})$$

where α is the absorption coefficient, h is the Planck constant, v is the light frequency, and A is a constant that is a function of the refractive index of the material.

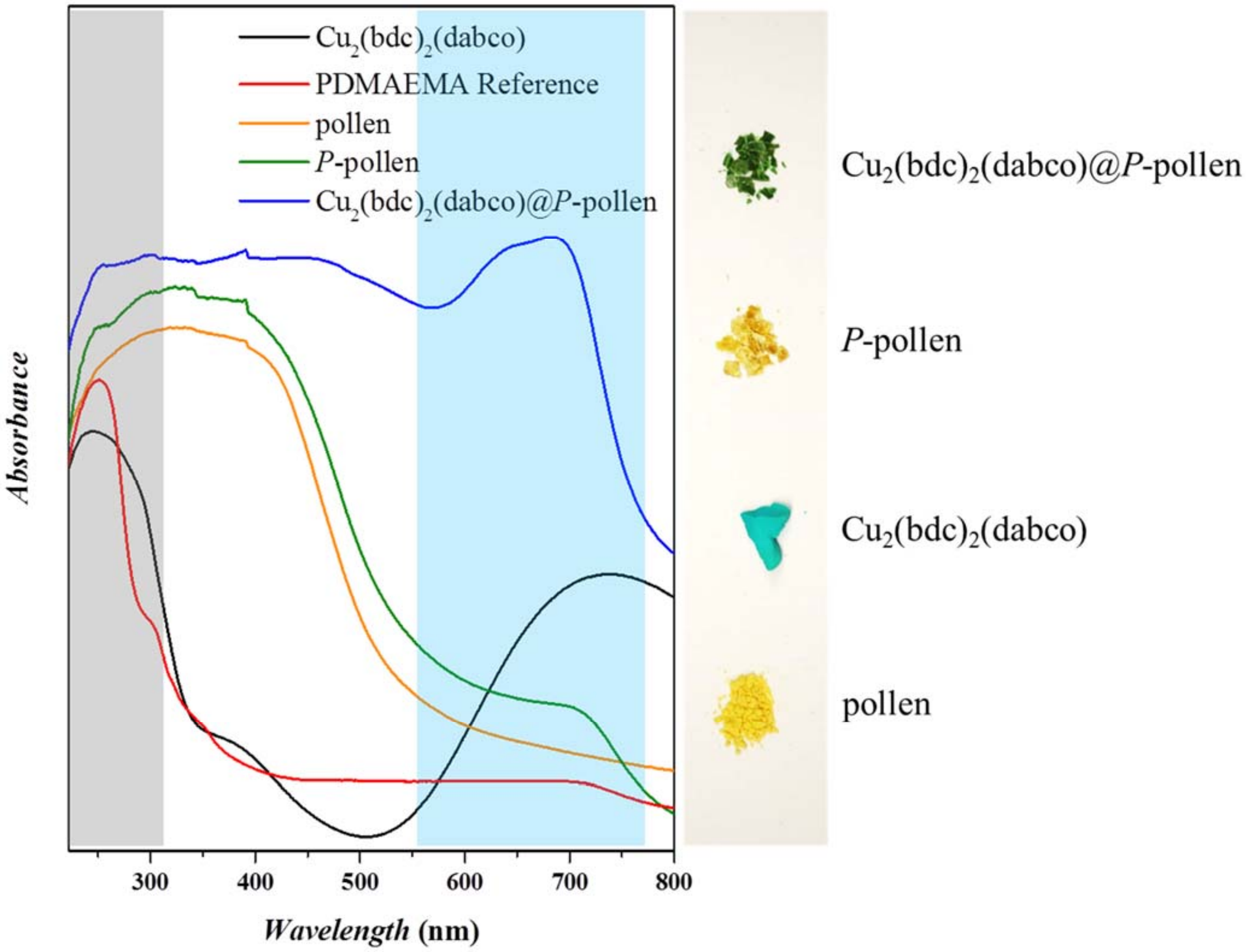

Figure S4. Ultraviolet-visible diffuse reflectance spectra of the Cu$_2$(bdc)$_2$(dabco) before and after incorporation in the *P*-pollen composite.

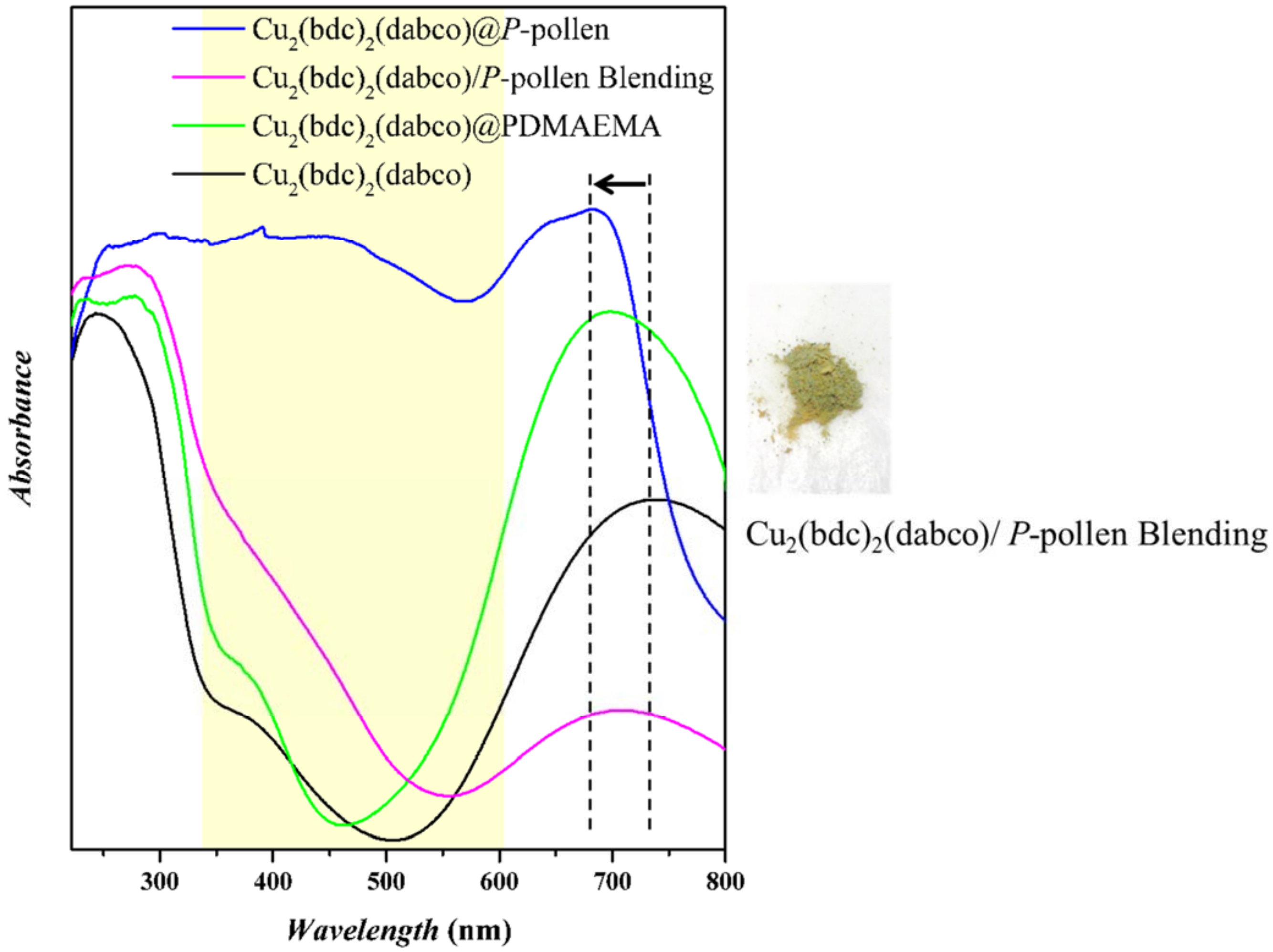

Figure S5. The comparison of ultraviolet-visible diffuse reflectance spectra of the Cu$_2$(bdc)$_2$(dabco) and *P*-pollen composites before (blending in solid state, Cu$_2$(bdc)$_2$(dabco)/*P*-pollen Blending) and after (interacting in solution state, Cu$_2$(bdc)$_2$(dabco)@*P*-pollen) association. Note: the blending ratio between Cu$_2$(bdc)$_2$(dabco) and *P*-pollen is the same as in Cu$_2$(bdc)$_2$(dabco)@*P*-pollen.

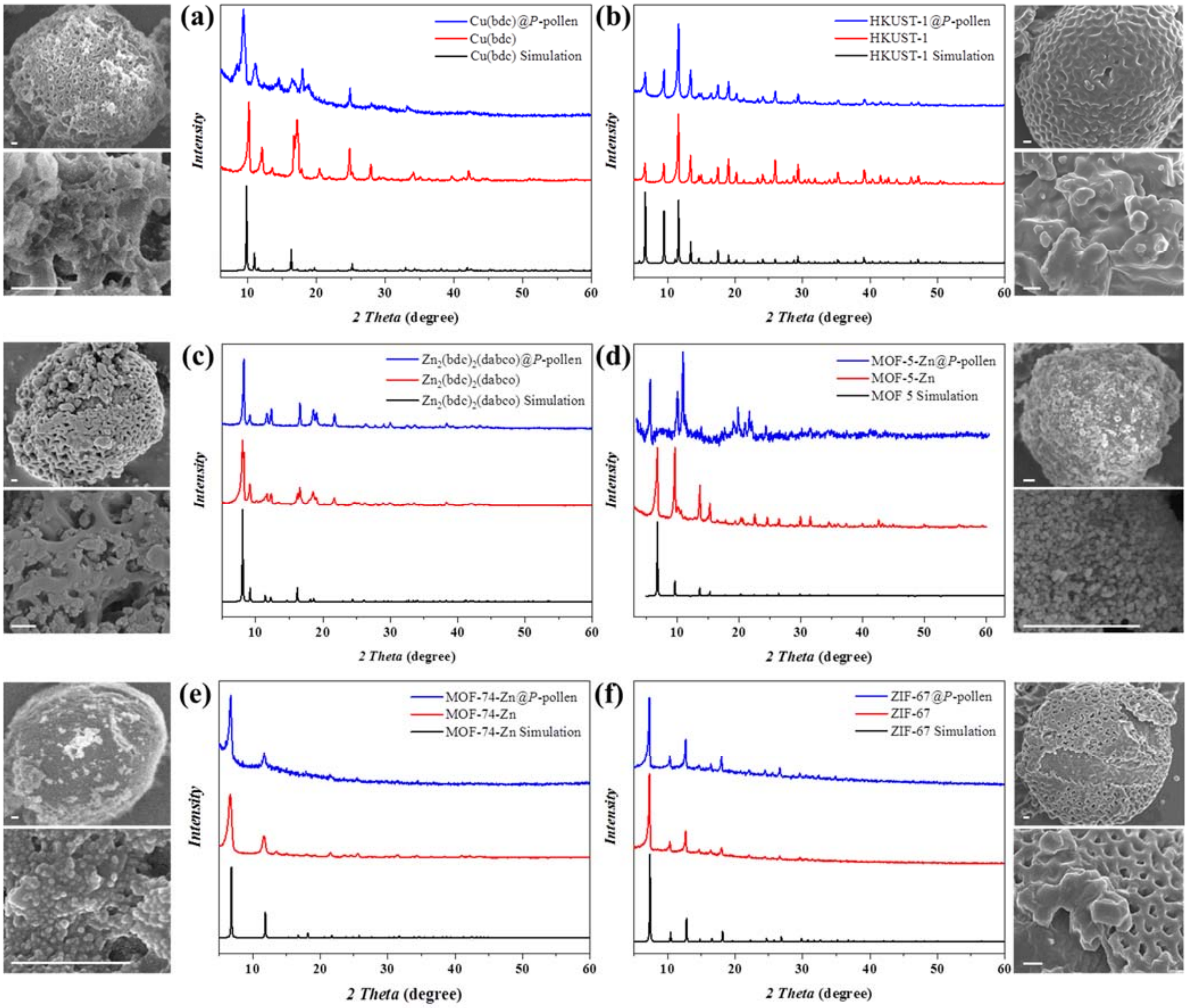

Figure S6. PXRD profiles of (a) Cu(bdc), (b) HKUST-1, (c) $Zn_2(bdc)_2(dabco)$, (d) MOF-5-Zn, (e) MOF-74-Zn and (f) ZIF-67 before and after incorporation in the *P*-pollen with simulated profiles as comparison. Corresponding SEM images of each MOF@*P*-pollen composite with the 1 µm scale bar, giving estimated nanocrystal size of Cu(bdc) ~200 nm, HKUST-1 ~500 nm, (c) $Zn_2(bdc)_2(dabco)$ ~500 nm, (d) MOF-5-Zn ~50 nm, (e) MOF-74-Zn ~50 nm and (f) ZIF-67 ~500 nm.

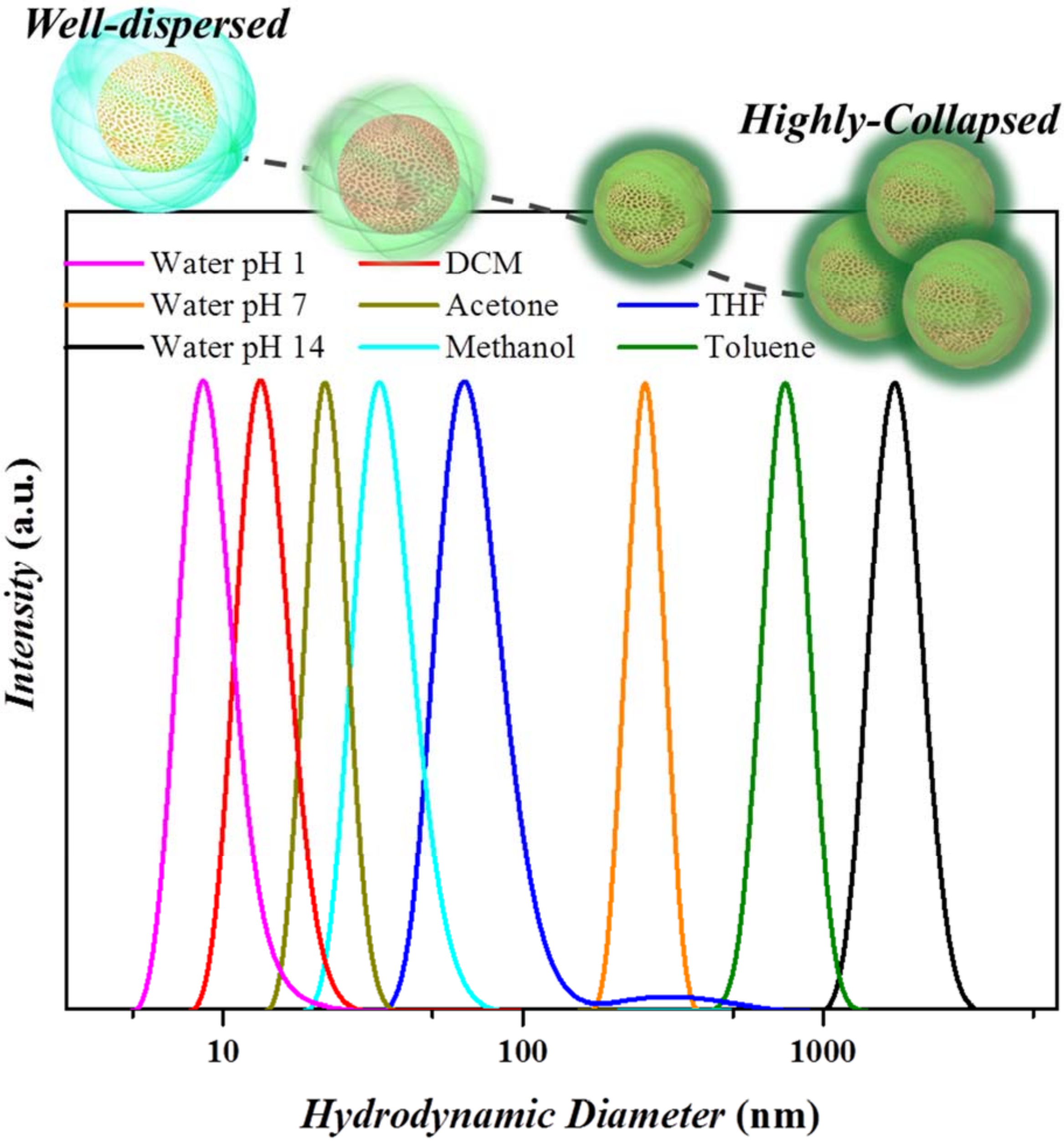

Figure S7. Solvent-induced particle size change of free-formed PDMAEMA determined by DLS in different solvents and pH values with speculated morphology of *P*-pollen. Note: DLS measurements were performed with PDMAEMA chains cut from the *P*-pollen.

The decreasing hydrodynamic diameter (*d*, nm) was correlated to the increasing solubility of PDMAEMA brushes in the applied solvent, *i.e.*, the smallest *d* was detected in acid and DCM (8.7 and 13.5 nm) due to the highly dissolved PDMAEMA chains, and the value became larger in water and toluene (255 and 712 nm) owing to the recoiled morphology. Severe aggregation was eventually observed when using basic solution (d = 1.7 μm).

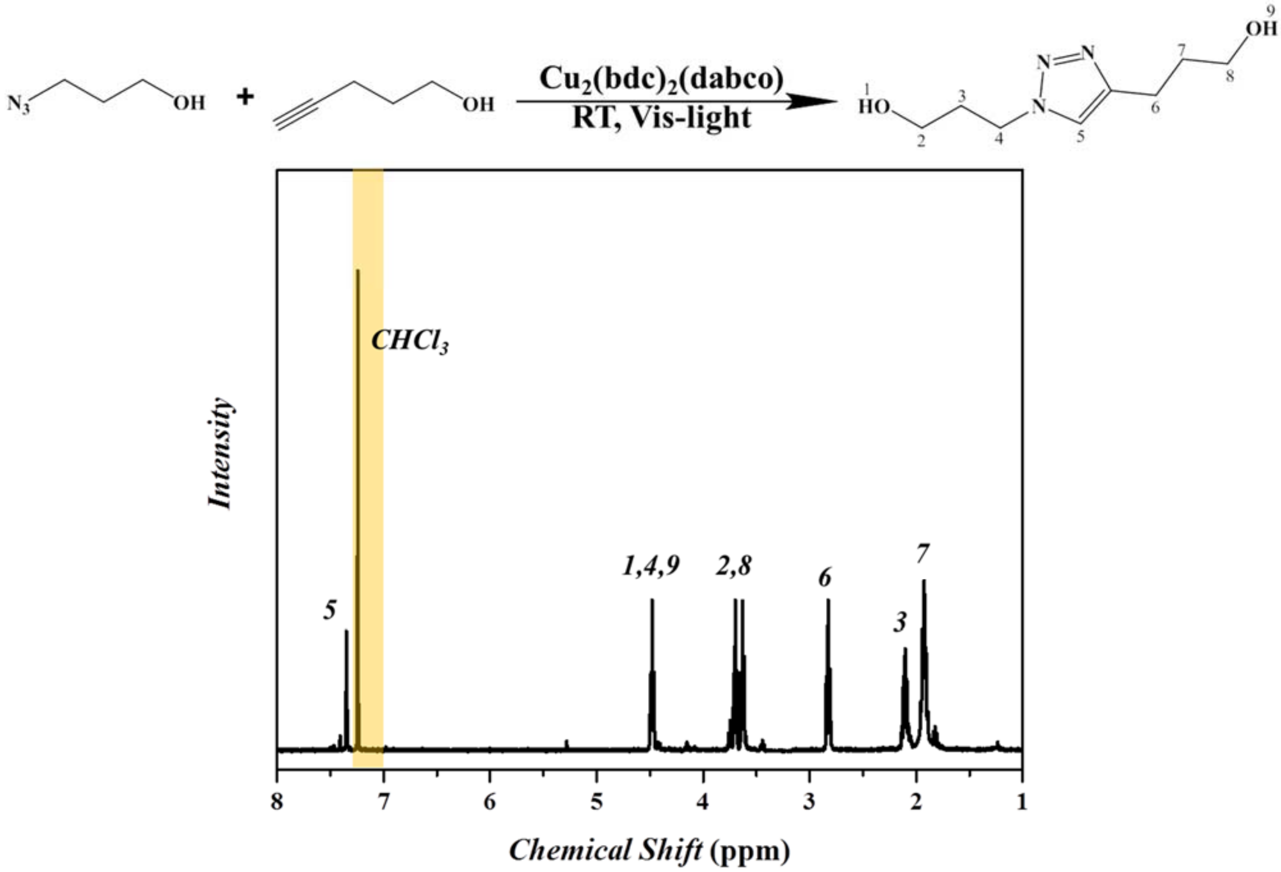

Figure S8. ^{1}H NMR of the as-synthesized triazole in chloroform-*d*.

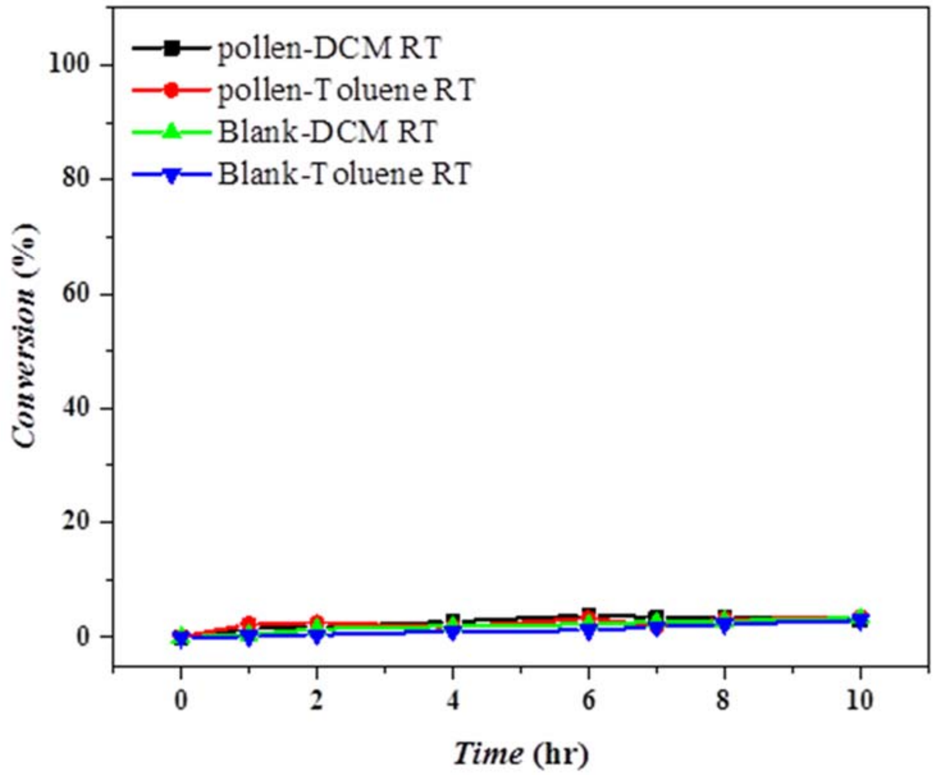

Figure S9. Evolution of conversion with time for photo-CuAAC reaction in DCM (D) or toluene (T) solution catalyzed via innate pollen only or without any catalyst.

Table S2. Summary of catalytic performance at ambient temperature [a]

Catalyst	Solvent	Conversion (%) [b]	TON [c]	TOF (h^{-1}) [d]
$Cu_2(bdc)_2(dabco)$	Toluene	50.4	1133.3	113.3
	DCM	33.1	742.7	74.3
	Methanol	27.3	614	61.4
	THF	24.9	560	56.0
$Cu_2(bdc)_2(dabco)$@*P*-pollen	Toluene	10.4	235.6	23.6
	DCM	92.5	2077.8	207.8
	Methanol	32.3	726	72.6
	THF	21.7	488	48.8
$Cu_2(bdc)_2(dabco)$ @PDMAEMA	Toluene	22.3	499.6	50.0
	DCM	23.7	532.9	53.3

[a] The reaction was carried out at ambient temperature under visible light using Cu amount of 0.446 mg in each type of catalyst. [b] The conversion at 10 h was utilized. [c] TON = turn over number, which was calculated based on the product amount after 10 h (wt%) and comprised amount of Cu ion in the mixture (wt%). [d] TOF = turn over frequency, which was calculated based on the TON at 10 h.

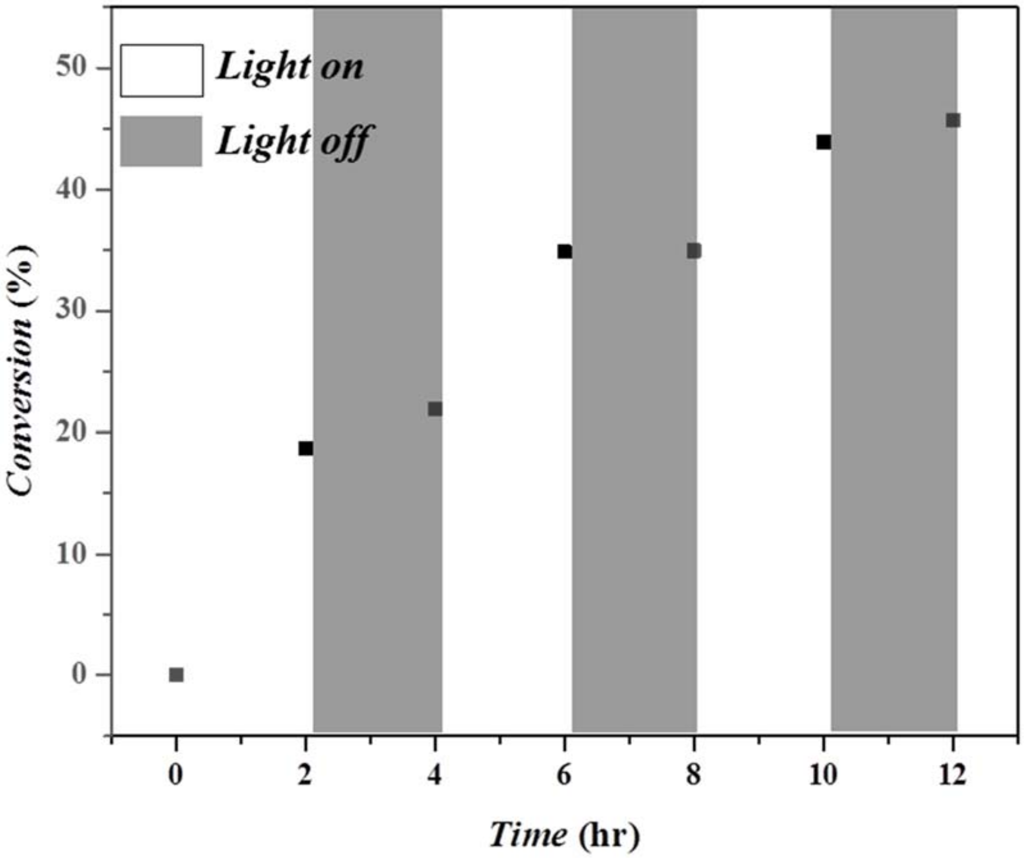

Figure S10. Demonstration of temporal control through interlude light exposure: with consecutive light (white area) and dark treatment (shaded area).

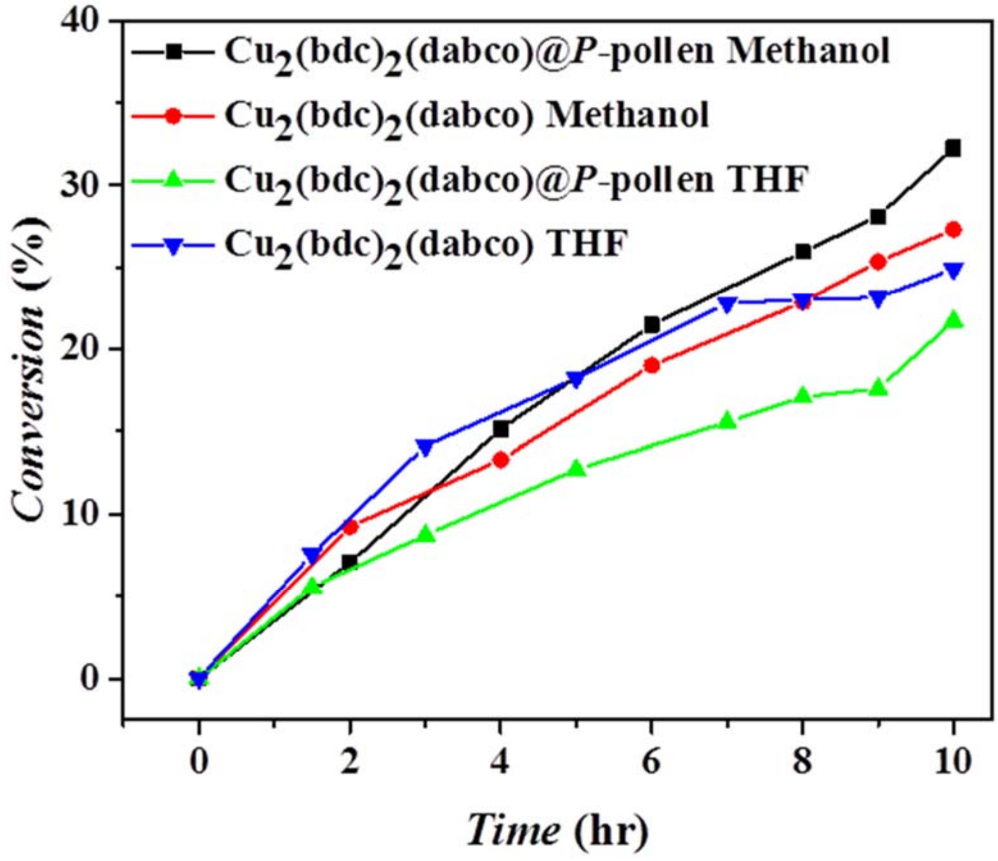

Figure S11. Evolution of conversion with time for photo-CuAAC reaction in methanol or THF solution catalyzed via innate $Cu_2(bdc)_2(dabco)$ or $Cu_2(bdc)_2(dabco)$@*P*-pollen.

Table S3. Residual Cu concentration (mg/g) in the click products synthesized via different catalytic composites. [a]

	Initial Bulk (mg/g)[b]	Product (mg/g)[c]
$Cu_2(bdc)_2(dabco)$	0.45	0.017 (16.9 ppm)
$Cu_2(bdc)_2(dabco)$ @PDMAEMA	0.45	0.016 (15.8 ppm)
$Cu_2(bdc)_2(dabco)$@*P*-pollen	0.45	0.012 (10.5 ppm)

[a] Determined *via* ICP-OES. [b] The theoretical Cu amount in the initial bulk solution. The initial bulk contains the same amount of Cu ion contributed by different catalytic composites. [c] The as-synthesized click product was dissolved in methanol, and the suspension was isolated *via* centrifugation to remove the catalytic composites. After drying by vacuum, the product was analyzed by ICP-OES.

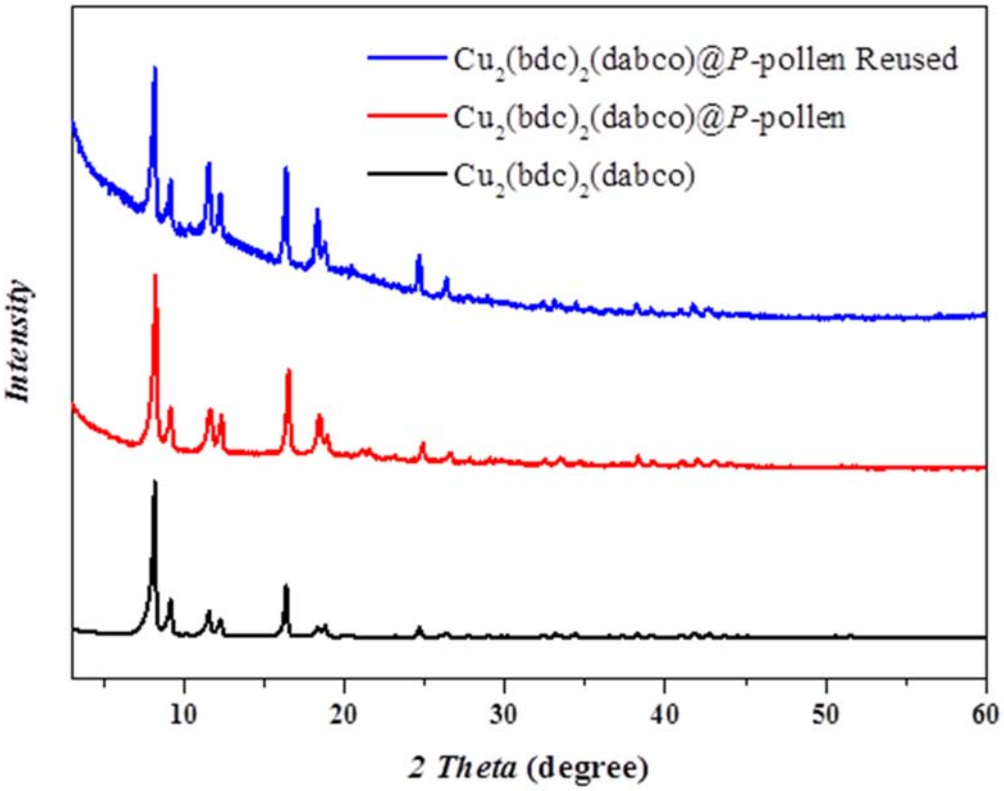

Figure S12. PXRD profile of $Cu_2(bdc)_2(dabco)$@*P*-pollen after catalyzing click reaction in on/off reusability for 6 times (3 cycles).

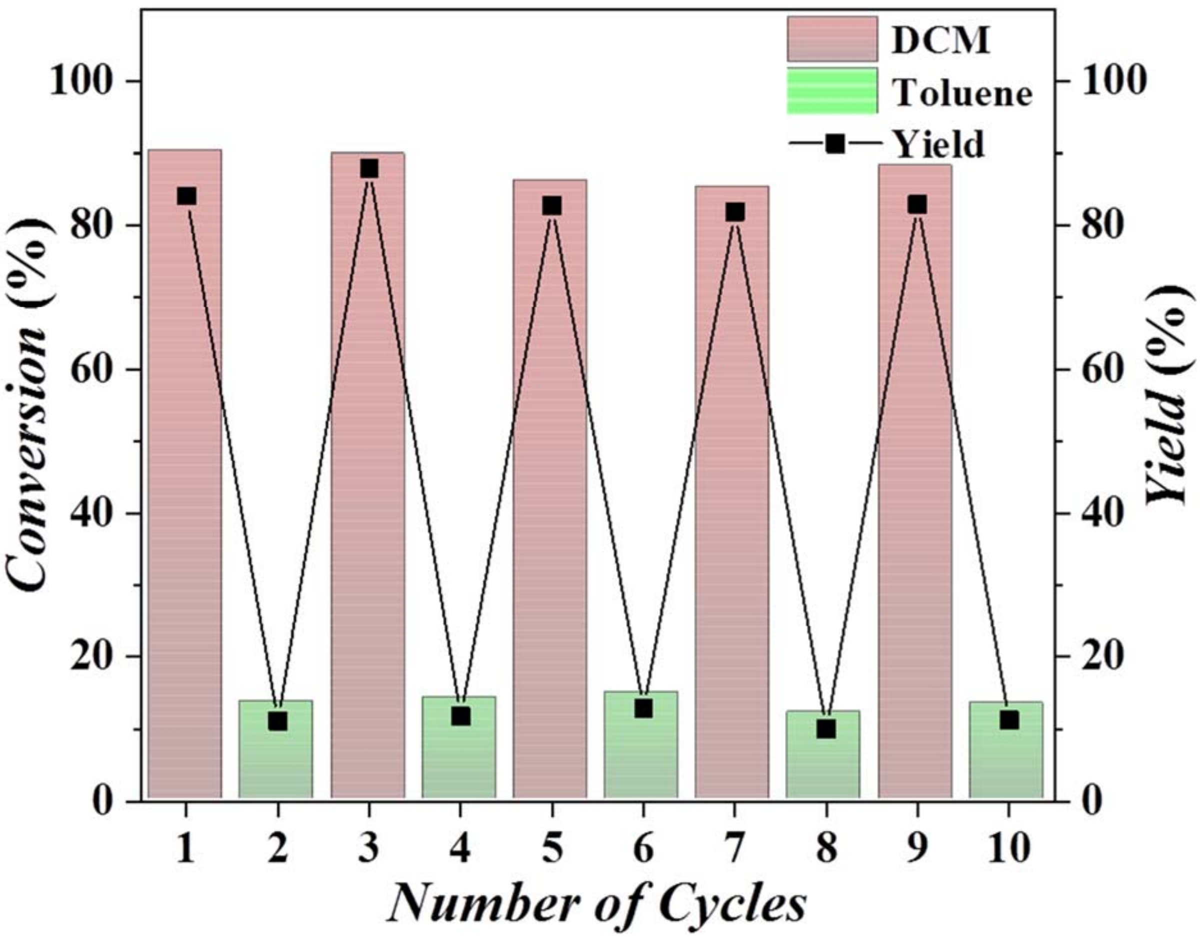

Figure S13. The five-cycle on-off catalytic reusability as extension of Figure 4b.

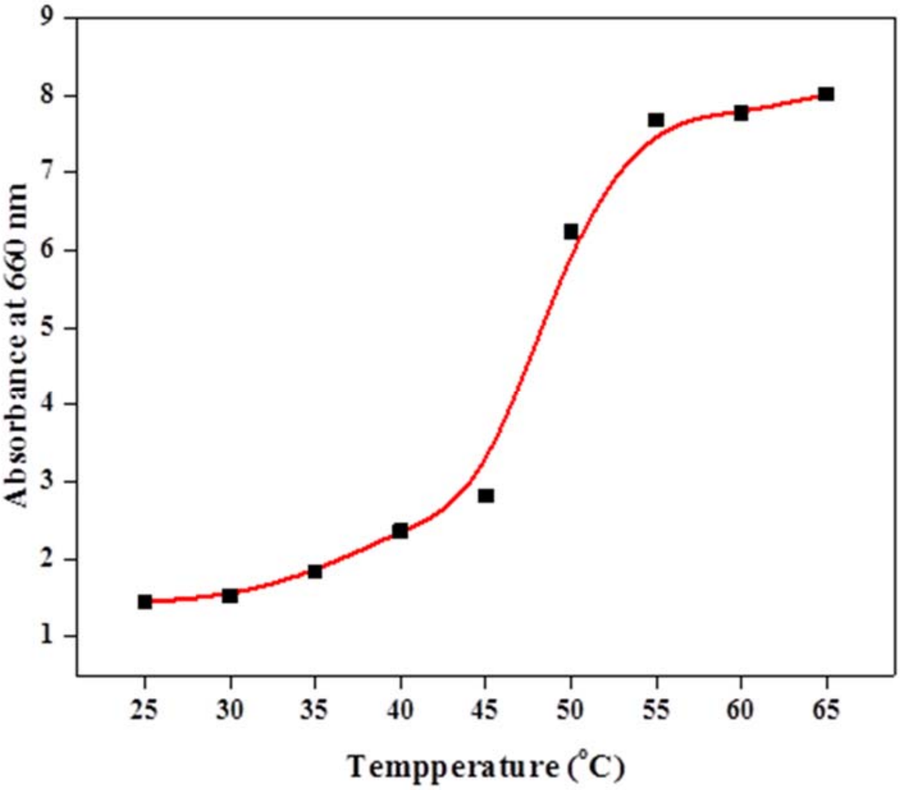

Figure S14. Temperature-dependent turbidity curves of PDMAEMA cut from *P*-pollen: 1 wt % in click reagents with DCM, using UV-vis spectroscopy at 660 nm.

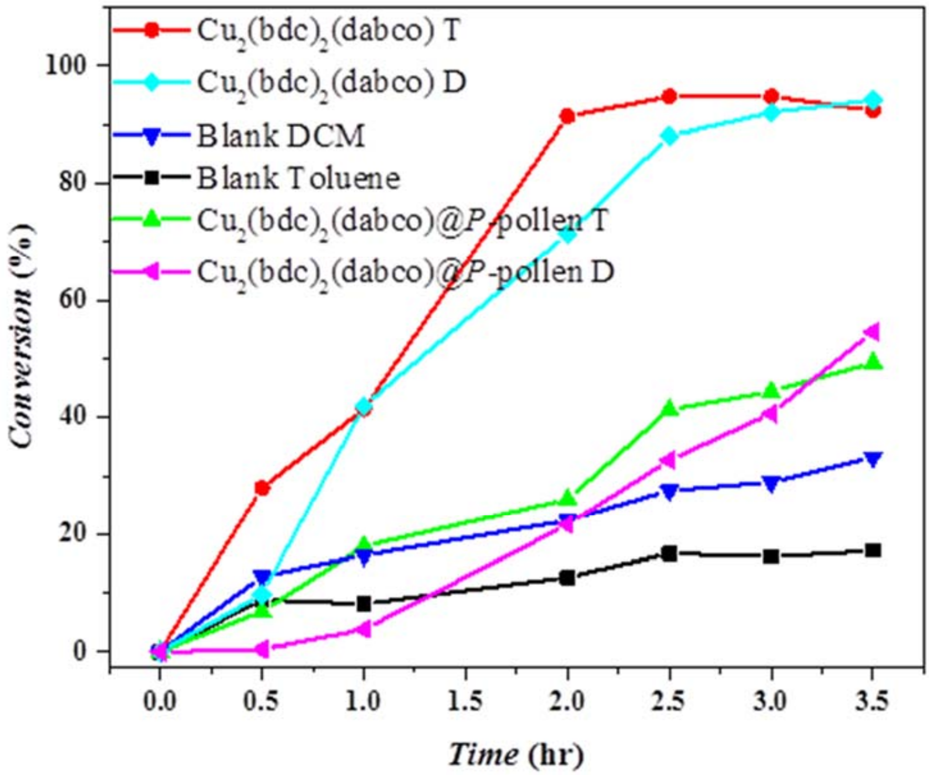

Figure S15. Evolution of conversion with time for photo-CuAAC reaction in DCM (D) or toluene (T) solution catalyzed via various $Cu_2(bdc)_2(dabco)$ composites at 65 ºC.

Table S4. Summary of catalytic performance at 65 ºC under visible light [a]

Catalyst	Solvent	Conversion (%) [b]	TON [c]	TOF (h^{-1}) [d]
$Cu_2(bdc)_2(dabco)$	Toluene	91.4	2055.7	1027.9
	DCM	71.4	1604.3	802.1
$Cu_2(bdc)_2(dabco)$@*P*-pollen	Toluene	25.9	583.9	291.9
	DCM	21.6	486.1	243.1

[a] The reaction was carried out at a 65 ºC under visible light using Cu amount of 0.446 mg in each type of catalyst. [b] The conversion at 2 h was utilized. [c] TON = turn over number , which was calculated based on the product amount after 2 h (wt%) and comprised amount of Cu in the mixture (wt%). [d] TOF = turn over frequency , which was calculated based on the TON at 2 h.

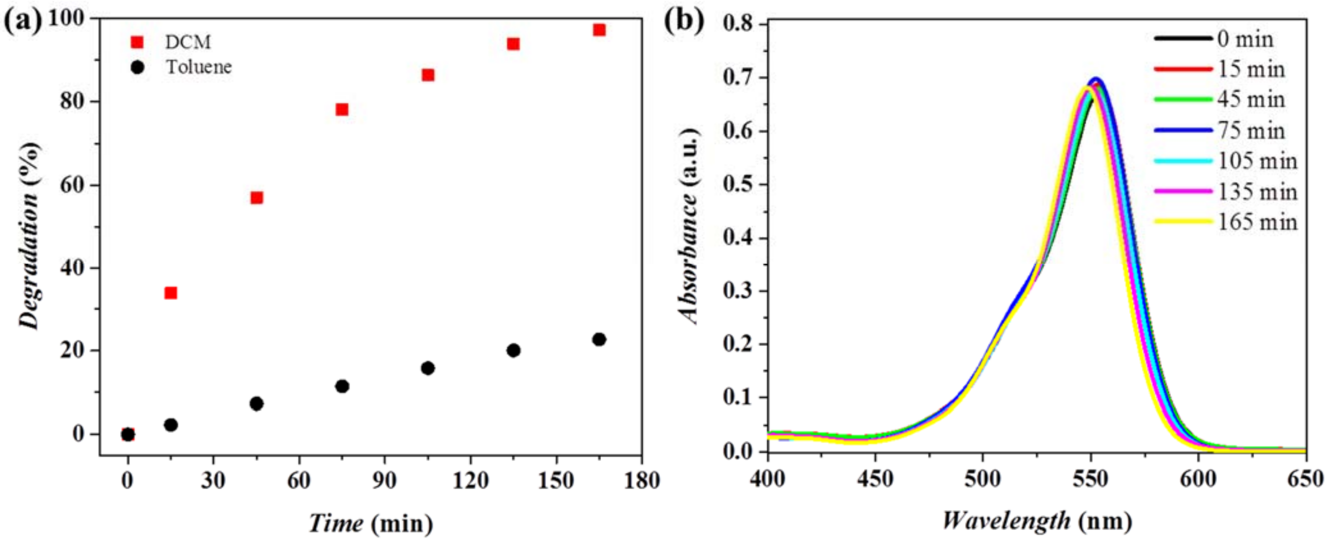

Figure S16. The solvent-dependent degradation of RhB by $Cu_2(bdc)_2(dabco)$@*P*-pollen in (a) DCM or toluene illuminated under visible light and (b) in DCM in the dark treatment at ambient temperature.

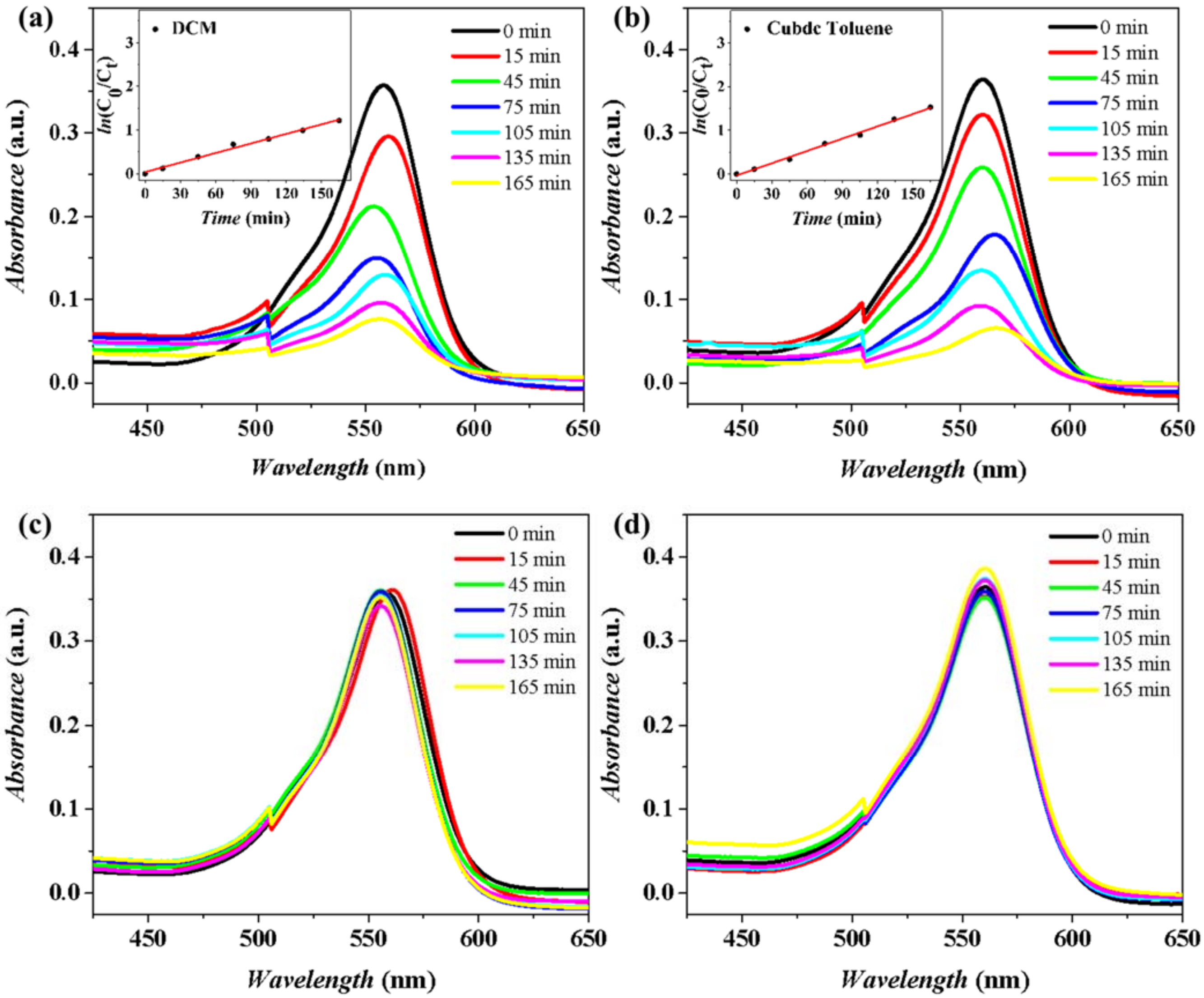

Figure S17. UV-vis spectra following RhB decomposition at ambient temperature under visible light: catalyzed by $Cu_2(bdc)_2(dabco)$ in (a) DCM and (b) toluene; blank condition with *P*-pollen in (c) DCM and (d) toluene without MOF catalyst. The inset indicates the linear time-dependent semilogarithmic plots during the whole reaction.

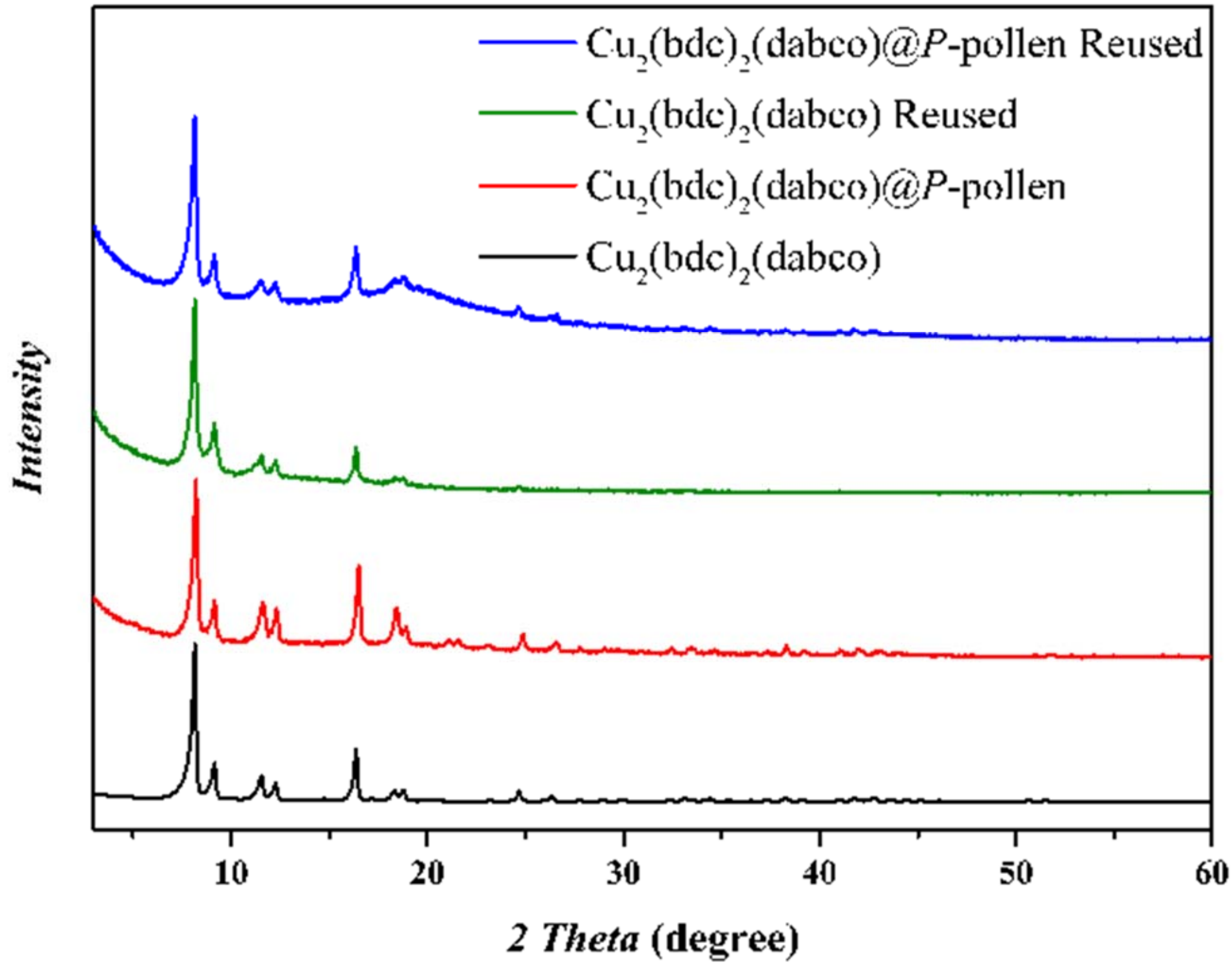

Figure S18. PXRD profile of Cu$_2$(bdc)$_2$(dabco) and Cu$_2$(bdc)$_2$(dabco)@*P*-pollen after catalyzing the photodegradation of Rhodamine B.

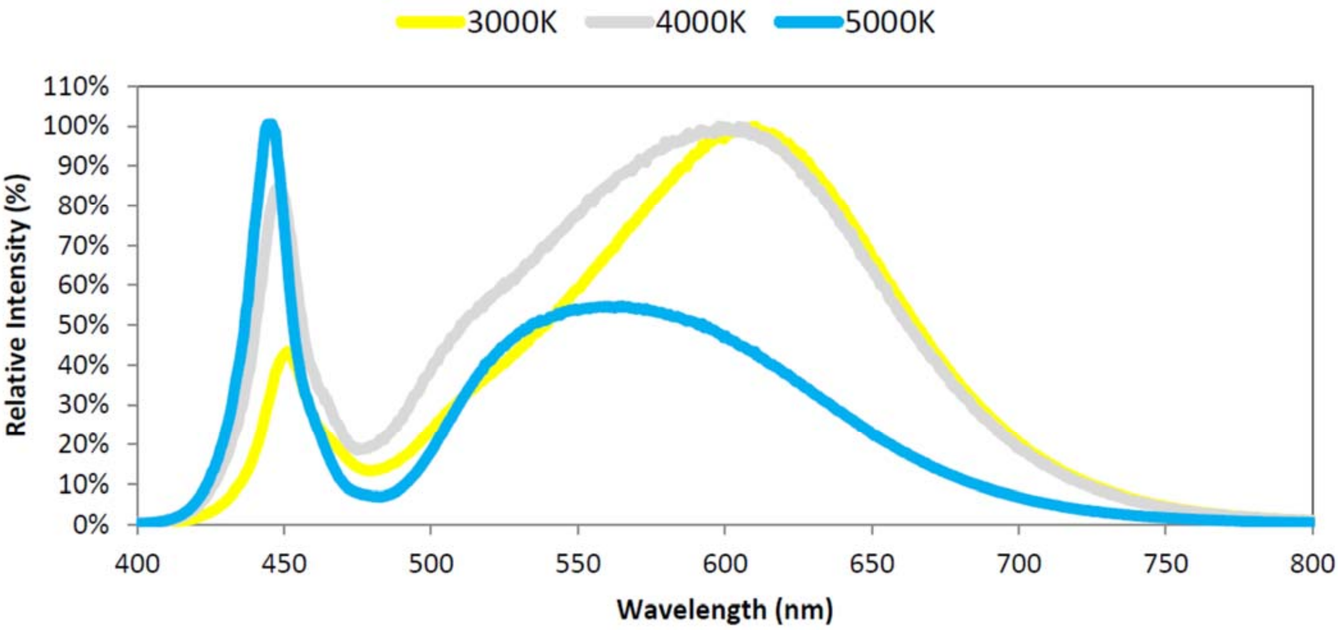

Figure S19. The emission spectrum of the visible-light source applied in this study. Note: the spectra were analyzed under rated current with junction temperature at 25 °C; spectrum for warm white is 3000 K and 80 color rendering index (CRI); spectrum for neutral white is 4000 K and 80 CRI; spectrum for cool white is 5000 K and 70 CRI. (source of information: www.bridgelux.com)

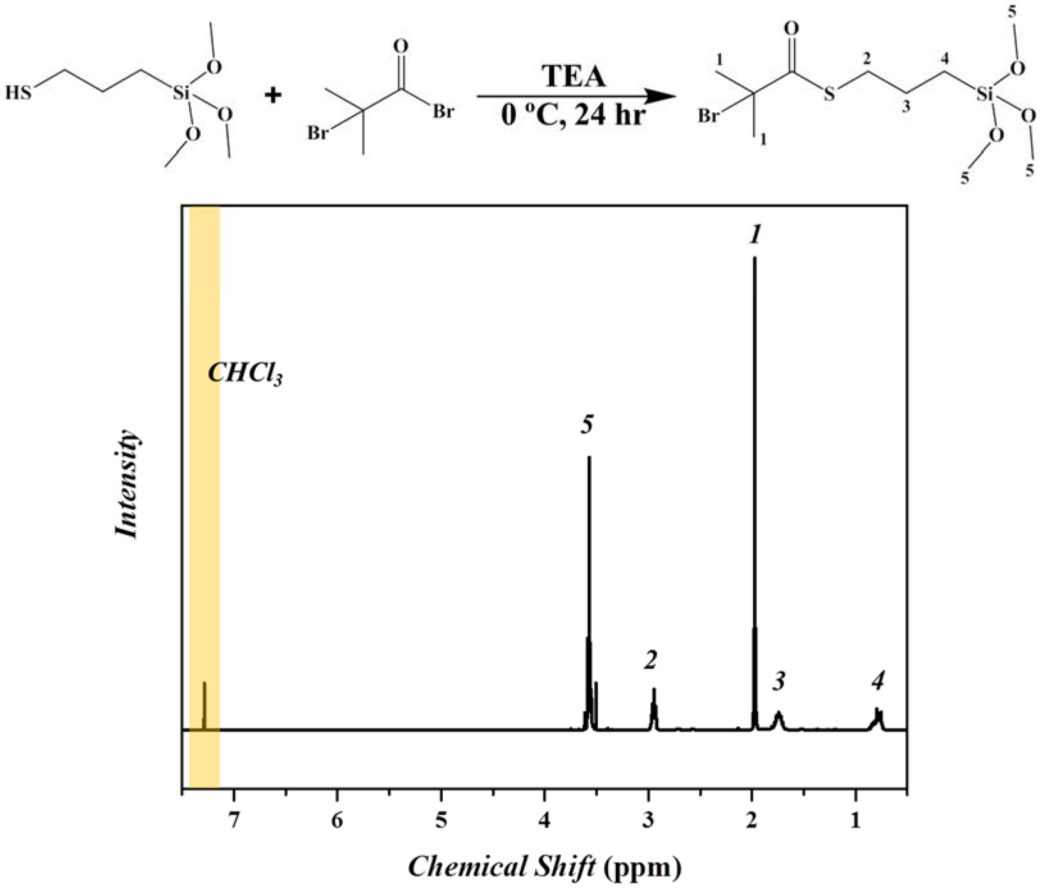

Figure S20. ^{1}H NMR of the synthesized MPTS-Br in chloroform-*d*.

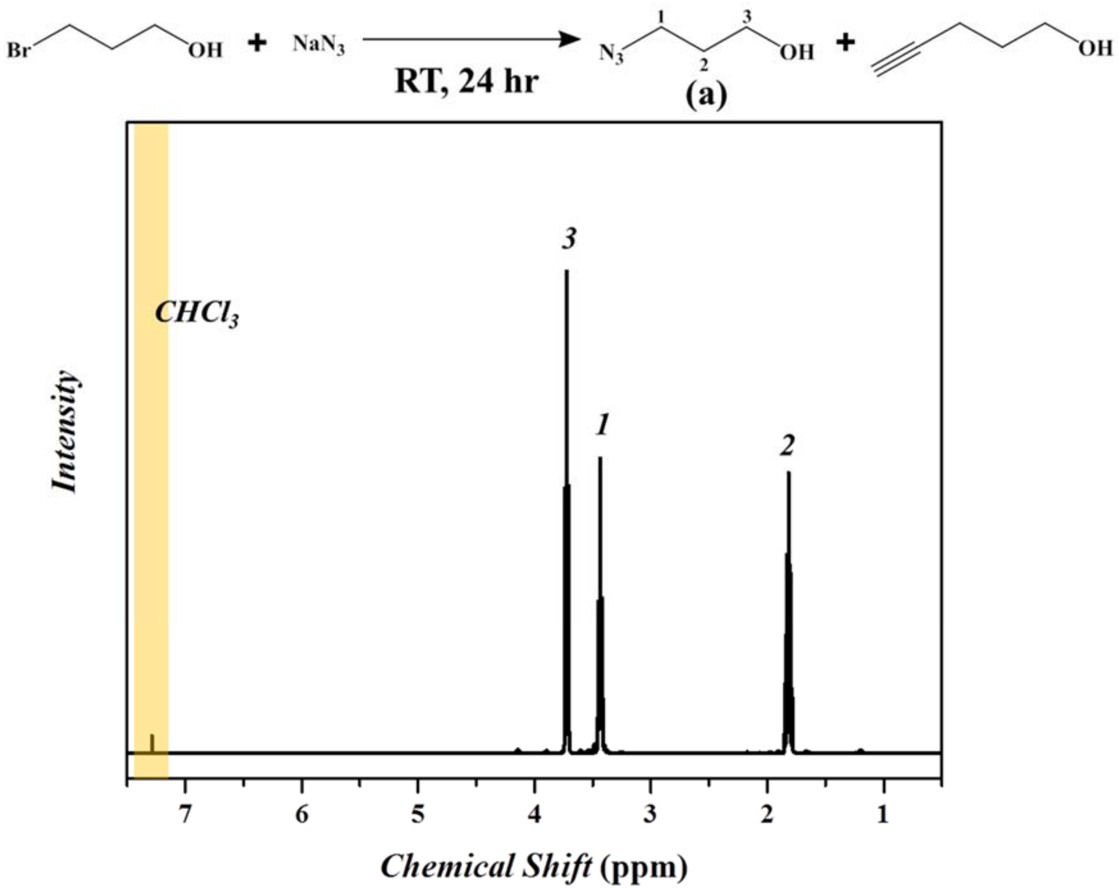

Figure S21. ^{1}H NMR of the synthesized 3-azido-1-propanol in chloroform-*d*.

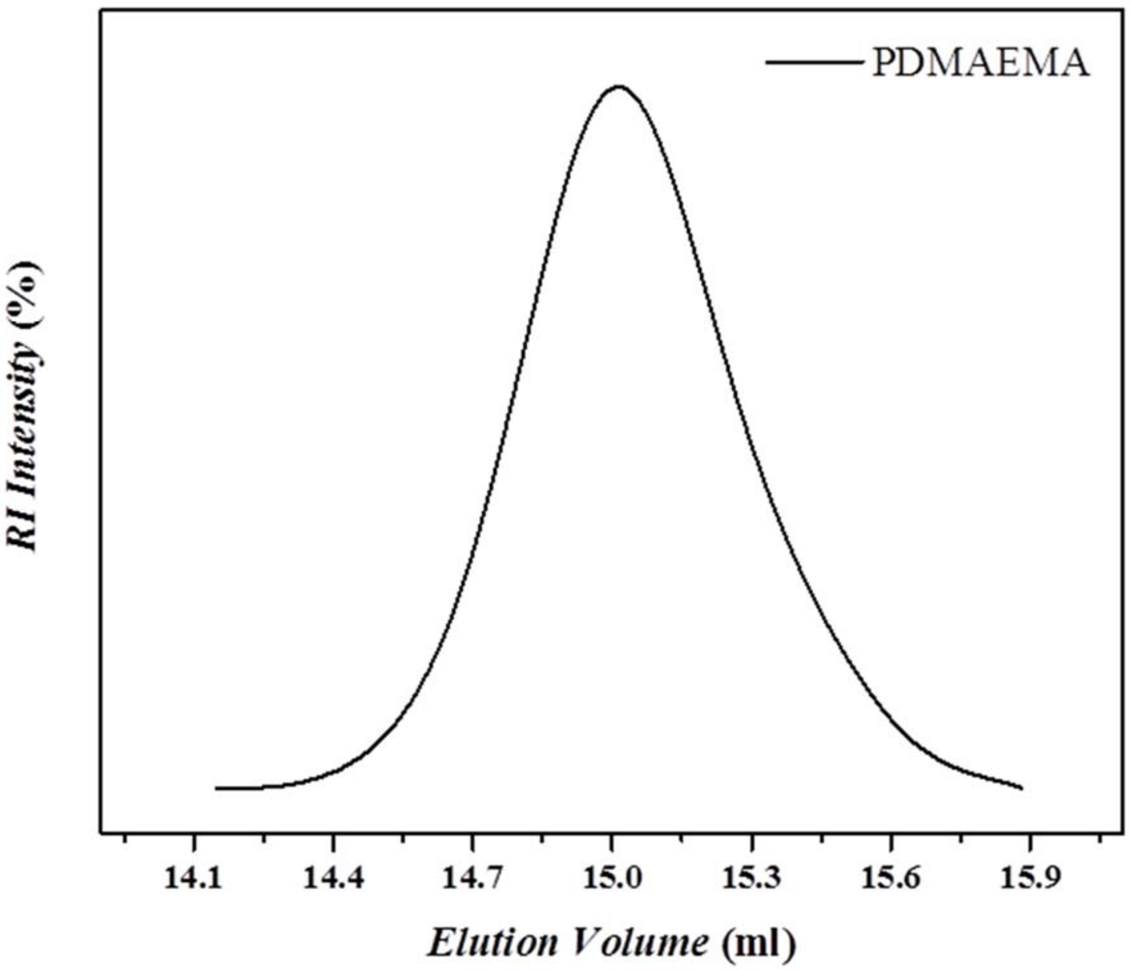

Figure S22. SEC chromatogram of the grafted PDMAEMA cut from *P*-pollen, giving M_{n} = 67800 g/mol and *Đ* = 1.2.

References:

1. O. O. Fadiran and J. C. Meredith, *J. Mater. Chem. A*, 2014, **2**, 17031-17040.
2. H.-C. Lee, H.-Y. Hsueh, U. S. Jeng and R.-M. Ho, *Macromolecules*, 2014, **47**, 3041-3051.
3. S. R. Gondi, A. P. Vogt and B. S. Sumerlin, *Macromolecules*, 2007, **40**, 474-481.
4. J. Willersinn, A. Bogomolova, M. B. Cabré and B. V. K. J. Schmidt, *Polym. Chem.*, 2017, **8**, 1244-1254.
5. H.-C. Lee, M. Antonietti and B. V. K. J. Schmidt, *Polym. Chem.*, 2016, **7**, 7199-7203.
6. B.-Q. Ma, K. L. Mulfort and J. T. Hupp, *Inorg. Chem.*, 2005, **44**, 4912-4914.
7. D. J. Tranchemontagne, J. R. Hunt and O. M. Yaghi, *Tetrahedron*, 2008, **64**, 8553-8557.
8. H. Li, M. Eddaoudi, M. O'Keeffe and O. M. Yaghi, *Nature*, 1999, **402**, 276.
9. B. Panella and M. Hirscher, *Adv. Mater.*, 2005, **17**, 538-541.
10. C. G. Carson, K. Hardcastle, J. Schwartz, X. Liu, C. Hoffmann, R. A. Gerhardt and R. Tannenbaum, *Eur. J. Inorg. Chem.*, 2009, **2009**, 2338-2343.
11. H. K. Kim, W. S. Yun, M.-B. Kim, J. Y. Kim, Y.-S. Bae, J. Lee and N. C. Jeong, *J. Am. Chem. Soc.*, 2015, **137**, 10009-10015.
12. J. Qian, F. Sun and L. Qin, *Mater. Lett.*, 2012, **82**, 220-223.
13. J. Zhuang, W. Dai, Q. Tian, Z. Li, L. Xie, J. Wang, P. Liu, X. Shi and D. Wang, *Langmuir*, 2010, **26**, 9686-9694.
14. J. Tang, V. Etacheri and V. G. Pol, *Sci. Rep.*, 2016, **6**, 20290.
15. Y. Xia, W. Zhang, Z. Xiao, H. Huang, H. Zeng, X. Chen, F. Chen, Y. Gan and X. Tao, *J. Mater. Chem.*, 2012, **22**, 9209-9215.
16. L. C. H. Moh, M. D. Losego and P. V. Braun, *Langmuir*, 2011, **27**, 3698-3702.
17. M. W. Hahn, D. Abadzic and C. R. O'Melia, *Environ. Sci. Technol.*, 2004, **38**, 5915-5924.
18. J. I. Langford and A. J. C. Wilson, *J. Appl. Crystallogr.*, 1978, **11**, 102-113.
19. H. Borchert, E. V. Shevchenko, A. Robert, I. Mekis, A. Kornowski, G. Grübel and H. Weller, *Langmuir*, 2005, **21**, 1931-1936.